

The Influence of Radiosonde “Age” on TRMM Field Campaign Soundings Humidity Correction

BISWADEV ROY

Science Systems and Applications, Inc., and Mesoscale Processes Branch, NASA GSFC, Greenbelt, Maryland

JEFFREY B. HALVERSON

Joint Center for Earth Systems Technology, University of Maryland, Baltimore County, Baltimore, and Mesoscale Processes Branch, NASA GSFC, Greenbelt, Maryland

JUNHONG WANG

Atmospheric Technology Division, National Center for Atmospheric Research, Boulder, Colorado

(Manuscript received 25 November 2002, in final form 11 July 2003)

ABSTRACT

Hundreds of Vaisala sondes with an RS80-H Humicap thin-film capacitor humidity sensor were launched during the Tropical Rainfall Measuring Mission (TRMM) field campaigns (1999) Large Scale Biosphere–Atmosphere (LBA) experiment held in Brazil and the Kwajalein Experiment (KWAJEX) held in the Republic of the Marshall Islands. Six humidity error correction algorithms were used primarily for applying system-bias correction to RS80-H humidity data. All TRMM field campaign Vaisala humidity soundings were corrected for dry bias using this algorithm. An overall improvement of 3% RH for daytime and 5% RH for nighttime soundings was achieved. Sonde age was ascertained using respective serial numbers (in this case the range is 0.06–2.07 yr) and used in the algorithm for calculation of sensor aging error and chemical contamination errors. Chemical contamination error is also found to be a dominant error source. Daytime sensor-arm heating for the first 50 s of the sonde launch is found to bear a cosine variation with sonde age. Surface reference temperature and sonde registered surface temperature are both used for calculating surface saturation vapor pressure, which in turn is used for sensor-arm-heating error estimation during the first 50 s. Site-mean CAPE values are found to increase significantly after correction. It is suggested that sonde surface temperature error must also be corrected for sonde age while using the present RS80-H correction algorithm. An age–height plot of the differences between the uncorrected and corrected specific humidity value for all Vaisala soundings shows an age-dependent increase (approximately 3.4 g kg^{-1} for 2-yr-old sondes). Variation of specific humidity difference was not found to be very significant for the upper levels when the sensor is less than 1.25 yr old.

1. Introduction

During the Tropical Rainfall Measuring Mission (TRMM) field campaigns a combined total of 709 Vaisala radiosondes were launched at the Large Scale Biosphere–Atmosphere (LBA) experiment fixed sites Rebio-Jaru and Rolim de Moura in Brazil, and at the Kwajalein Experiment (KWAJEX) fixed but floating site—the National Oceanic and Atmospheric Administration (NOAA) research vessel *Ron H. Brown*, hereafter called R/V *RHB* (see Figs. 1a,b). One important TRMM-LBA objective was to study mean thermodynamic and kinematic airmass properties of wet season (1 January–

28 February 1999) convection over Rondonia, Brazil. The TRMM-LBA sounding array shown in Fig. 1b was located about 2400 km northwest of Rio de Janeiro. KWAJEX soundings were obtained during July–September 1999 and were taken in the Republic of Marshall Islands sites located about 1300 km east of Guam. All fixed-site stations launched eight sondes per day (at 0000, 0300, 0600, 0900, 1200, 1500, 1800, and 2100 UTC). These soundings have undergone preliminary quality control for general use by the scientific community. An overview of the procedures adopted for quality control of TRMM field campaign soundings is presented in Roy and Halverson (2002). LBA radiosonde launch time was converted from UTC to local time by subtracting 5 h from UTC time stamps. Similarly, the KWAJEX radiosonde local time of launch was calculated by adding 12 h to the UTC time stamp. We expect that the corrected soundings will provide im-

Corresponding author address: Dr. Biswadev Roy, U.S. EPA, MEARB/Atmospheric Modeling Division, 109 T. W. Alexander Drive, Research Triangle Park, NC 27711.
E-mail: Roy.Dev@EPA.gov

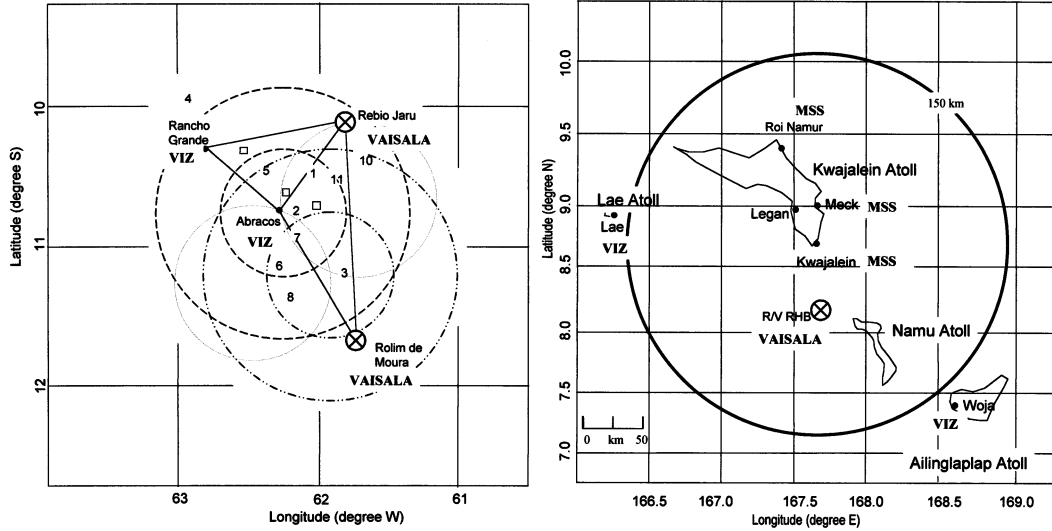


FIG. 1. TRMM-LBA and KWAJEX sounding arrays showing the sounding stations and type of sonde used. The Vaisala sites are marked with X inside a circle. (a) Locations of Rebio-Jaru and Rolim de Moura Vaisala sounding sites shown with respect to all other sounding sites using the VIZ sonde in Rondonia, Brazil. Circles over the sounding array represent various radar masks. (b) Location of R/V RHB Vaisala sounding site during KWAJEX at approximately 8.36°N, 67.73°E.

proved latent heating budgets in the Tropics, especially when compared with model-derived and satellite estimates. These soundings may also be useful for studying the characteristics of convective systems (see Halverson et al. 2002). Sounding-derived convective available potential energy (CAPE) is an important environmental stability parameter required for studying characteristics of convective systems as well as for studies related to

understanding of continental cloud structure and electrification (Williams et al. 2002).

A large dry bias in the Vaisala sounding humidity profile of Rebio-Jaru was observed when the mean profile was compared with a similar one derived using coincident VIZ sonde humidity soundings taken at a nearby LBA station, Abracos (see Fig. 2). A systematic and significant dry bias in Vaisala soundings was also ob-

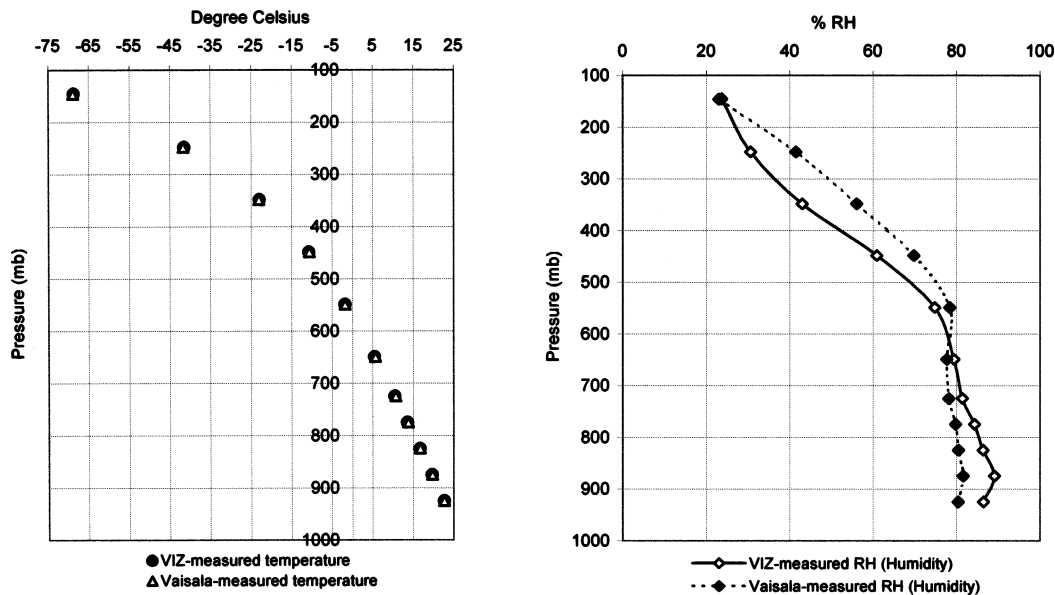


FIG. 2. A comparison plot showing mean profiles from Vaisala and VIZ sondes of (a) mean temperature and (b) RH profiles derived after averaging specific humidity for coincident soundings. Note the reversal of the mean RH bias in the midlevel.

served by Zipser and Johnson (1998) in the data obtained from the Tropical Ocean Global Atmosphere Coupled Ocean–Atmosphere Response Experiment (TOGA COARE) conducted in 1992 and 1993.

To correct the biases observed in TRMM soundings we used the empirical polynomial fits and regression equations based on the National Center for Atmospheric Research/Atmospheric Technology Division (NCAR/ATD) series of laboratory tests as reported in Wang et al. (2002, hereafter referred to as W02). We found a consistently good response from application of the algorithm to the present set of soundings. Humidity soundings are corrected by applying the equations for the temperature-dependence model, modeled ground-check error, sensor aging error, chemical contamination, basic calibration, and daytime sensor-arm-heating error. The purpose of this paper is to evaluate the RS80-H correction algorithm after application to the TRMM soundings and also to report an age-dependent variation of the sensor-arm-heating error estimate that is used in the W02 algorithm based on Cole and Miller (1995). These evaluation results may be useful for development of a reference radiosonde system, as mentioned in Wang (2002). In section 2 of this paper we describe the RS80-H sensor and how the data were obtained during the TRMM field campaigns. Section 3 describes the procedure adopted for correcting the Vaisala RH dry bias and the assumptions that we made. Generally it was thought that the sensor-arm-heating biases are independent of the sonde age, but after application of the correction procedure we have found an inherent age dependence. A brief description and interpretation of the results obtained after sensor-arm-heating correction are presented in section 4. An overall improvement in the RH data is obtained after applying the W02 algorithm. A brief discussion about the resulting data quality based on the improved site-mean CAPE values, and an age–height plot of the specific humidity differences, is also given in section 4. In section 5 we have summarized the results and made a few suggestions for future work.

2. Sensor and data description

During the TRMM field campaign, radiosonde relative humidity was measured using the thin-film capacitive hygristor RS80-H. This H-type thin-film humidity sensor was developed by Vaisala and was subsequently introduced for atmospheric use during the late 1980s. Water-vapor absorption by the polymer layer changes its capacitance, which in turn is calibrated to known RH value. Characteristics of the polymer layer depend on its capability of taking up water and its stability at higher humidity. The H-type sensor has reduced hysteresis and is more stable (as mentioned in W02) at higher humidity than its A-type predecessor, which uses a different polymer film. The main source of chemical contamination is the packaging material (a Mylar foil bag) that out-gasses onto the polymer, resulting in occupation of bind-

ing sites by nonwater molecules. This inhibits water-vapor absorption and affects the sensing characteristics of the hygristor. The RS80-H polymer also reacts to contamination due to the presence of the styrofoam radiosonde case and plastic components (W02). The hygristor measures in the range of 0%–100% RH with a 1% resolution. This sensor has a lag time of 1 s with 6 m s⁻¹ flow at 1000 mb and +20°C temperature. Sondes used during the TRMM field campaigns had an ascension rate of about 5–6 m s⁻¹ for the first few hundred meters above ground level. Data were obtained using the DigiCORA II model MW-15 ground system and processor. Ground-check (GC) parameters are typically measured using an independent set of instruments at the surface. The GC parameters are not used to adjust the sounding's factory-determined calibration coefficients. For the case of R/V *RHB* launches, an independent integrated suite for Improved Meteorological Instruments (IMET), as described in Hosom et al. (1995), was used at the surface for obtaining 1-min average data at sonde launch time. Calibration was done by feeding in a punched-hole strip during the GC procedure. The GC parameters (pressure, temperature, RH, wind speed, and wind direction) are then entered, and offsets are computed and recorded in the sounding data file. For the LBA launches at Rebio-Jaru and Rolim de Moura, a hand-held psychrometer, thermometer, and wind-measuring instrument was used for GC purposes. The Vaisala RH sensor samples approximately every 1.5 s. A least squares technique is then used to generate smoothed soundings at 10-s temporal resolution. This is done by the Vaisala sounding processing algorithm itself. We attempt to introduce system-bias correction to these 10-s interpolated data using the current algorithm.

There are 297 soundings from R/V *RHB* in the period between 25 July and 11 September 1999. The sondes were launched every 3 h continuously from R/V *RHB* but were disrupted during the period 19–27 August 1999 due to movement of the ship to other locations for logistic reasons. All R/V *RHB* data were reformatted to a consistent LBA format (Roy and Halverson 2002). There were 412 soundings performed at the LBA sites Rebio-Jaru and Rolim de Moura. Full-time operations at the two sites did not begin until 24 January 1999. Operations were terminated at Rolim de Moura on 21 February 1999 because the equipment was moved to another site. Operations were terminated at Rebio-Jaru on 25 February 1999. The raw data were subjected to a visual check procedure and the skew T – $\log p$ charts were generated for each sounding and were visually inspected to find errors in the data such as superadiabatic lapse rates and low-level temperature and humidity problems. A few other problems, such as rapid drying and rapid heating or cooling, were identified and corrected. Preliminary quality flagging of the datasets was performed, and version “d” files were created using a method similar to the TOGA COARE quality-flagging

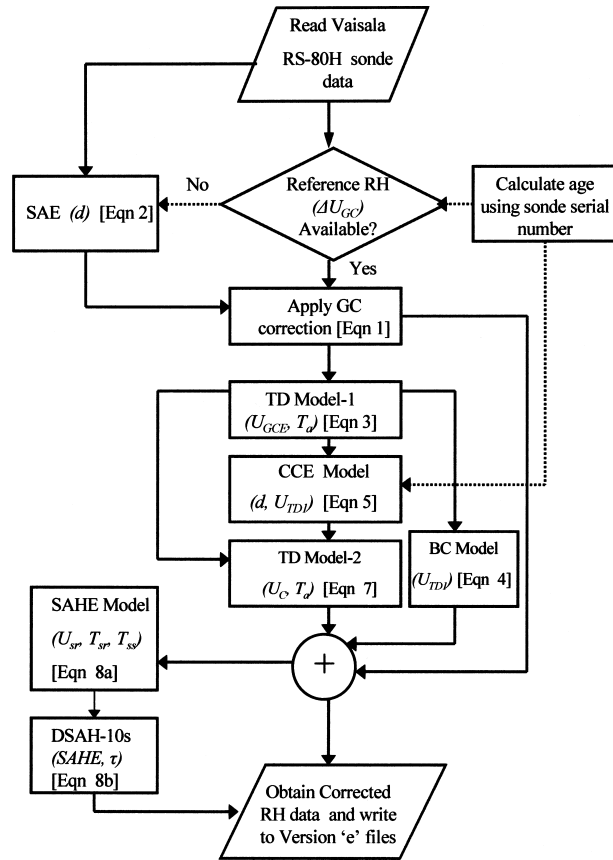


FIG. 3. The system-bias correction algorithm flowchart based on W02. The parameters in parentheses (in italics) are designated as the independent variable(s) on which the correction model referred to in each block depends. The dotted line represents the flow of sonde age data computed using the sonde serial number.

algorithm, as mentioned in Loehrer et al. (1996). The NCAR/ATD algorithm mentioned in W02 for RS80-H correction was applied to these version d files. Missing data have been flagged but no attempt was made to substitute missing data with any other estimate.

3. Method

An overview of the correction algorithm is given in Fig. 10 of W02, and a simplified flow diagram showing the entire correction procedure is given herein (Fig. 3).

a. Ground-check error correction

The GC error correction was performed using Eqs. (4)–(10) of W02

$$U_{\text{GCE}} = U_m - \Delta U'_{\text{GC}}, \quad (1)$$

where U_m is the radiosonde-measured RH (%) and $\Delta U'_{\text{GC}}$ is the GC error (GCE) measured using a test chamber, an independent instrument, and sonde-measured RH (%) at the surface.

b. Sensor aging error

Wherever GCE values were not recorded we used the modeled-GC values given by the sensor aging error (SAE). This error is caused by reduced polymer sensitivity to water vapor that grows with age (d) of the sensor. Following is the expression for calculation of age-dependent SAE (%) [based on Eq. (4-11H) of W02]:

$$\text{SAE} = -0.1638 + 1.4766d - 0.2257d^2, \quad (2)$$

where the age of the sensor is counted in years from the date of manufacture and may be accurately calculated using the sonde serial number. The resulting GCE is added to the entire sounding.

c. Ambient-temperature-dependent humidity correction model 1

After performing suitable GC correction using either the measured or modeled GC error as described above, an ambient temperature (T_a) dependent correction model (TD1) based on Eq. (5-1H) of W02 was applied to the GCE-corrected RH data (U_{GCE}). The resulting RH value (%) is used for calculation of basic-calibration error and chemical contamination humidity error, mentioned in sections 3d and 3e:

$$\begin{aligned} U_{\text{TD1}} = & -0.61 + 0.9561U_{\text{GCE}} + (0.031 + 0.00359U_{\text{GCE}})T_a \\ & + (-0.00033 - 0.0000727U_{\text{GCE}})T_a^2 \\ & + [0.0000014 - (9.6E - 8)U_{\text{GCE}}]T_a^3 \\ & + [(-3.1E - 09) + (5.431E - 09)U_{\text{GCE}}]T_a^4. \end{aligned} \quad (3)$$

d. Basic-calibration-model-derived error

Vaisala RH sensors are individually calibrated against a reference during the production process; hence, each sensor is measured against a reference. For this purpose an average basic-calibration model is fitted through the sensor's calibration points. Each new sensor is checked using an average model, so there is every likelihood that an error is introduced during this basic-calibration (BC) procedure. W02 used a test chamber to generate reference RH values and ascertained actual error due to application of the average BC model. They introduced a polynomial fit [Eq. (4-6H) of W02] to the test RH data in order to calculate the BC model error (BCE) (%) for the RS80-H:

$$\text{BCE} = H_0 + H_1U_{\text{TD1}} + H_2U_{\text{TD1}}^2 + H_3U_{\text{TD1}}^3, \quad (4)$$

where

$$\begin{aligned} H_0 &= -0.3019, & H_1 &= -0.0081, \\ H_2 &= 0.0011, & \text{and } H_3 &= -1.23E - 05. \end{aligned}$$

e. Contamination correction model

The H-Humicap polymer sensor is contained in a vacuum-sealed Mylar foil bag that outgasses packaging material. This alters the polymer's water selectivity, resulting in a dry bias. W02 performed extensive laboratory work to ascertain the accuracy of heat treatment tests on 14 different batches of RS80 radiosonde materials aged between 0.46 and 6.1 yr. They also tested for other sources of contamination, such as plastic components and styrofoam radiosonde casing, while using various drying agents (desiccants) to note the sensor characteristics. Equation (4-1H) of W02 is a contamination correction (CC) model that calculates chemical contamination error (CCE) (%) as a function of sensor age (d) and temperature-dependence-model-corrected relative humidity (U_{TD1}):

CCE

$$= [kh_0 + (kh_1)d + (kh_2)(d^2) + (kh_3)(d^3) + (kh_4)(d^4)] \\ \times [ph_0 + (ph_1)(U_{TD1}) + (ph_2)(U_{TD1}^2) + (ph_3)(U_{TD1}^3)], \quad (5)$$

where

$$\begin{aligned} kh_0 &= 0.018\ 8\ 66, & kh_1 &= 1.978\ 206, \\ kh_2 &= -1.342\ 78, & kh_3 &= 0.369\ 157\ 24 \\ kh_4 &= -0.032\ 41, & ph_0 &= 1.6994, \\ ph_1 &= 0.1368, & ph_2 &= -0.0018, \text{ and} \\ ph_3 &= 1.4105E - 05. \end{aligned}$$

In the next step, BCE and CCE are added to U_{TD1} to get calibration- and contamination-error-corrected relative humidity (U_C) (%):

$$U_C = U_{TD1} + BCE + CCE. \quad (6)$$

f. Temperature-dependent model 2

The resulting relative humidity value (U_C) from (6) needs to be converted to an equivalent RH (%) at radiosonde-measured ambient temperature. Another temperature-dependent model [Eq. (5-2H) of W02, i.e., TD2] is used for this purpose:

$$U_{TD2} = \frac{U_C + 0.61 - 0.031T_a + 0.000\ 33T_a^2 + 0.000\ 001\ 4T_a^3 + (3.1E - 09)T_a^4}{0.9601 + 0.000\ 359T_a - 0.000\ 085T_a^2 + (9.3E - 08)T_a^3 + (6.931E - 09)T_a^4}. \quad (7)$$

The temperature dependence of sensors is nonlinear in nature. TD2 model error for RS80-H is more significant at temperatures below -20°C . W02 have performed saturation level tests using test RH data and fitted measured RH differences to ambient temperature to derive the above-mentioned TD2 model.

g. Sensor-arm-heating error estimation for daytime soundings

Most of the time the humidity sensor was stored inside a controlled-environment storage facility, but it was exposed to the outside environment for a few minutes before actual launch of the radiosonde. This subjected the humidity sensor to radiational heating that introduces sensor-arm-heating error (SAHE) in surface data. The RS80-H sensor arm has a time constant (τ) of 13 s (W02), and it is expected that the sensor will equilibrate (respond to environmental changes with minimum error) in a period of about 4τ . Since the radiosonde ascension rate in the lower levels is approximately $5\text{--}6\ \text{m s}^{-1}$, the arm-heating error is most prominent in the first 200–300 m and is expected to last until the sensor equilibrates completely. Equation (4-7) of W02 uses prelaunch sonde temperature ($^\circ\text{C}$) at surface (T_{ss}), an independently measured reference temperature ($^\circ\text{C}$) at

surface (T_{sr}), and surface reference relative humidity (U_{sr}) (%) to calculate SAHE (%):

$$\text{SAHE} = U_{sr} - \frac{U_{sr}e_s(T_{sr})}{e_s(T_{ss})} \quad (8a)$$

the saturation vapor pressures (mb) in Eq. (5), $e_s(T_{sr})$ and $e_s(T_{ss})$, are computed using the method mentioned in Bolton (1980). In order to apply SAHE corrections to soundings obtained within the first few hundred meters, the W02 algorithm uses an exponential function [Eq. (4-8) of W02] for calculating the magnitude of arm-heating correction. In our case we have 10-s interpolated data and have applied SAHE correction to soundings at each of the successive observed levels within the first 50 s (250–300 m above surface). This error in % RH is termed here as DSAH-10s (daytime sensor-arm-heating error calculated every 10 s):

$$\text{DSAH-10s} = (\text{SAHE})e^{-t_i/\tau}, \quad (8b)$$

where t_i is the time delay in seconds from the sonde launch (10, 20, 30, 40, and 50 s in our case). Five 10-s delay points are considered for computing the DSAH-10s; hence, the damping factor $\exp(-t_i/13)$ in (8b) ranges from 0.46 to 0.02. While computing the SAHE (or DSAH-10s) no model-based correction is imparted to the sonde surface RH value. The original first-level sounding is used. It is also assumed that there were no

occurrences of low-level inversion during the daytime. Since the sonde RH at 10 s and later are corrected using the W02 algorithm, it is expected that the error occurring in a well-mixed boundary layer (during daytime) will only be caused due to radiation-induced sensor-arm heating. Radiosonde-measured surface RH is used for computing the DSAH-10s for all the successive five levels because the sonde-measured surface mixing ratio is ideally considered to remain constant in the well-mixed boundary layer (Wallace and Hobbs 1977).

Finally, the overall daytime corrected RH value is obtained by adding the RH corrected for ambient temperature using the TD2 model (U_{TD2}) with the DSAH-10s:

$$U_{W02} = U_{TD2} + \text{DSAH-10s}. \quad (9)$$

4. Results

a. Overall RH correction

Average daytime and nighttime vertical profiles of the uncorrected RH (U_m) minus corrected RH (U_{W02}) values (the difference profile) are presented in Fig. 4, which shows nighttime and daytime difference profiles for each site. The difference profiles show negative values mostly. This means that more moisture is added to the soundings. The daytime corrections include SAHE modification to the first 50 s of the sounding or up to about 200–300 m above ground level. From Figs. 4a–c it is seen that W02 adds moisture to the nighttime boundary layer since the slope of the difference profile is negative within the first few hundred meters above ground level. During daytime it is expected that the boundary layer is well mixed, and from Fig. 4 it is noted that W02 maintains the positive gradient in the daytime difference profile within the boundary layer. These results are ideally expected. It is also observed from Figs. 4a and 4b that more moisture is added to the LBA soundings above the midlevel. By comparing Figs. 4a and 4b with 4c it is noted that the difference profile does not show abrupt change in the R/V *RHB* case; rather, the difference is almost constant with height. One of the reasons for large excursions in the LBA-sounding-derived difference profile above the midlevel is probably the large GCE correction. The GC errors at LBA sites were calculated using data from handheld instruments. The GCE model was more frequently used for LBA soundings than R/V *RHB* because of lack of GC data, whereas we used very stable IMET instrument data for computing GCE and SAHE for the R/V *RHB* case. Practices in storing, handling, and releasing radiosondes may be another source of error in the RH data (W02).

The correction algorithm (W02) employs CCE, TD1, and TD2 models, which are a function of age, as well as a few derived intermediate relative humidity values. Hence, explanation of the large excursion in the LBA difference profile remains beyond the scope of the pres-

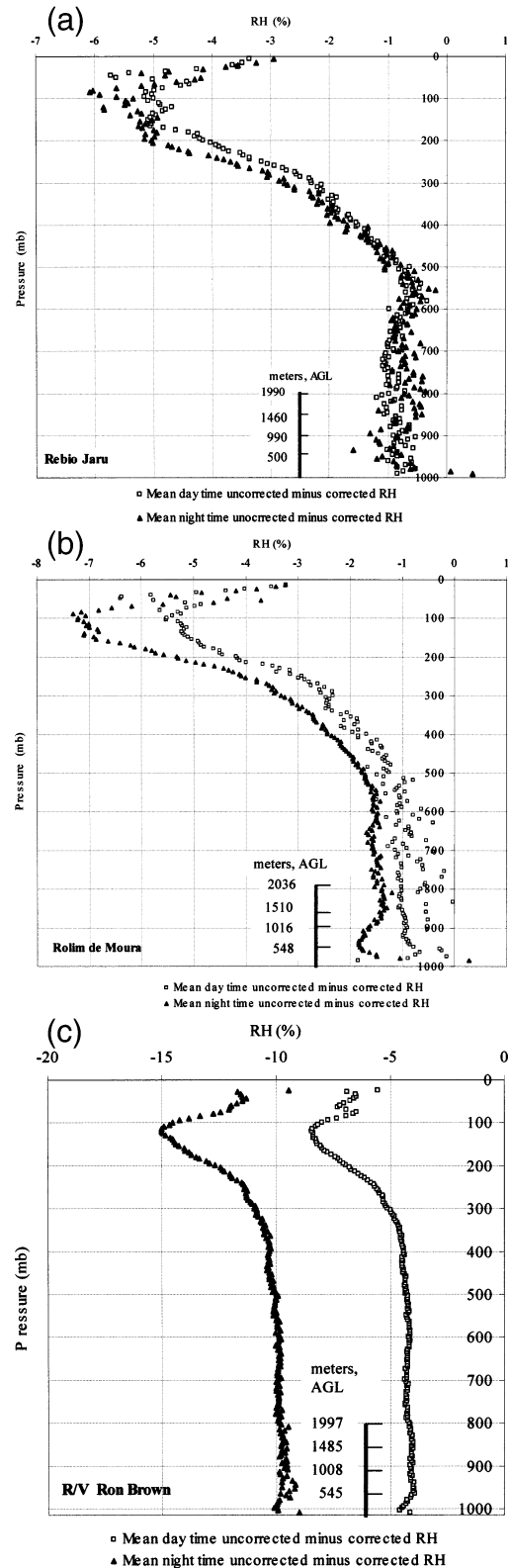


FIG. 4. Profiles of mean daytime and nighttime differences between the uncorrected and corrected RH data at the (a) Rebio-Jaru, (b) Rolim de-Moura, and (c) R/V *RHB* sites.

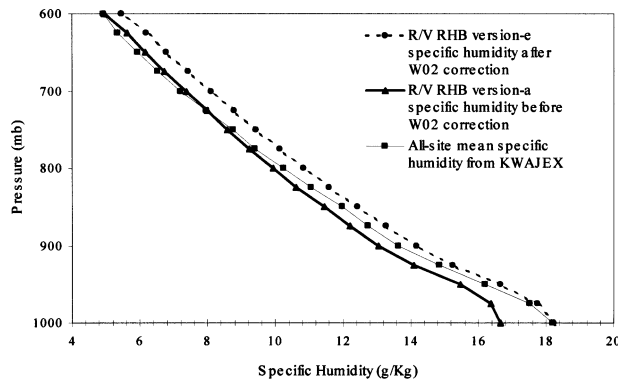


FIG. 5. Three specific-humidity profiles obtained using R/V *RHB* soundings: before correction, using version “a” data (thick line with triangles); all-site mean, using other VIZ and Aeromet’s Meteorological Sounding Systems (MSS; humidity data from Lae, Roi, Kwajalein, Meck, and Woja sites) (thin line with squares); and the W02-corrected humidity sounding (dashed line with circles).

ent study. It can also be inferred that, in general, the W02 algorithm introduces more moistening to the nighttime soundings than to the daytime cases. Ideally, the system should have moistened the lower levels and dried up the upper levels (cf. Figs. 2 and 4a).

In order to note changes in the RH data in the lower levels, we have plotted the mean R/V *RHB* specific humidity profile obtained after W02 correction along with uncorrected and KWAJEX site-mean specific humidity profiles (including soundings at the Lae, Roi, Kwajalein, Woja, and Meck sites). Figure 5 shows all three profiles together, drawn from surface up to the midlevel (600 mb). It is apparent from this figure that the W02 correction is more appropriate for the lower sounding levels because the corrected mean specific humidity profile is found to resemble more closely the site-mean profile.

b. Variation of mean correction parameters with sonde age

At the Rebio-Jaru site most of the observations were made with sondes in the age group 0.06–1.02 yr, and for the Rolim de Moura site most observations were made using sondes aged between 0.06–1.2 yr. There were a few sondes used at Rolim de Moura that were manufactured almost 2 yr prior to their use. Figures 6a and 6b give total counts of the 10-s Vaisala observations for various sonde ages at the Rebio-Jaru and Rolim de Moura sites, respectively. The R/V *RHB* observation counts for various age groups are not shown because the sondes were relatively new. Most observations made at the ship were obtained from sensors that were manufactured 0.19–0.33 yr prior to their use.

Figure 7 shows the variation of mean modeled GCE, CCE, BCE, SAHE, and the difference between uncorrected and W02-corrected humidity data ($U_m - U_{W02}$) with sonde age. Sixth-order polynomial fit (Press et al.

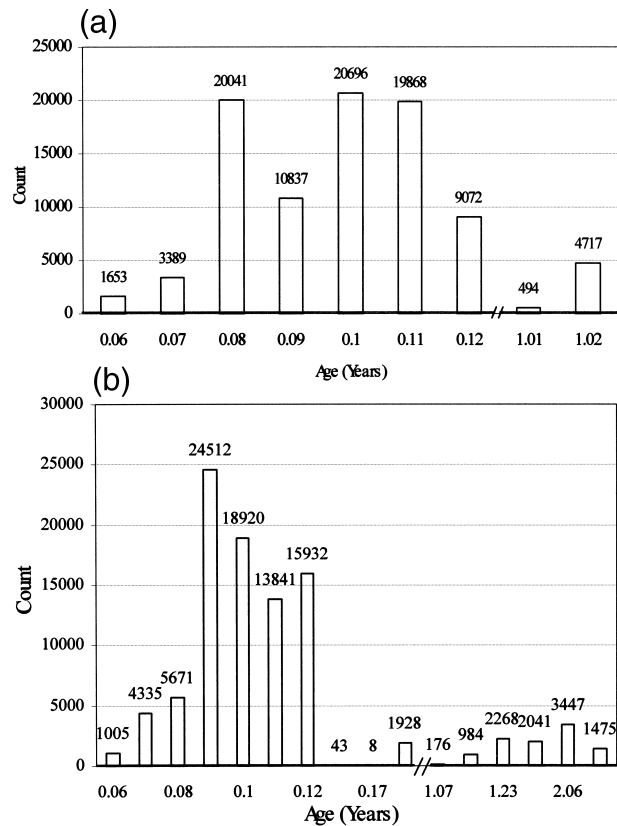


FIG. 6. Bar charts showing observation counts at various sonde ages for the (a) Rebio-Jaru and (b) Rolim de Moura sites.

1992) for each type of error is shown in Fig. 7. We have the following results: (i) the mean modeled GCE increases with age; (ii) the mean of CCE correction varies with age; (iii) the mean contamination, and mean DSAH-10s are found to vary in a cyclic manner with age. The CCE correction is noted to be minimum for about 1-yr-old sondes.

In this analysis we assume that there is no uncertainty involved in the sonde age determination procedure. However, W02 have reported that a 50% error in age introduces about a 45% error in CCE estimation. In the next section 4c we have investigated a possible reason why the SAHE and hence the DSAH-10s vary in a cyclic fashion with sonde age.

c. Variation of SAHE with age

SAHE is the relative humidity error at surface calculated using surface measurements, whereas DSAH-10s is the extension of SAHE at local levels above ground, separated by 10-s intervals and computed using (8b). Figure 8a shows the age-dependent variation of mean SAHE and DSAH-10s using all three stations’ daytime soundings. The points are mostly clustered in the age group 0.1–1.2 yr. There were only two sondes launched during the daytime that were more than 2 yr

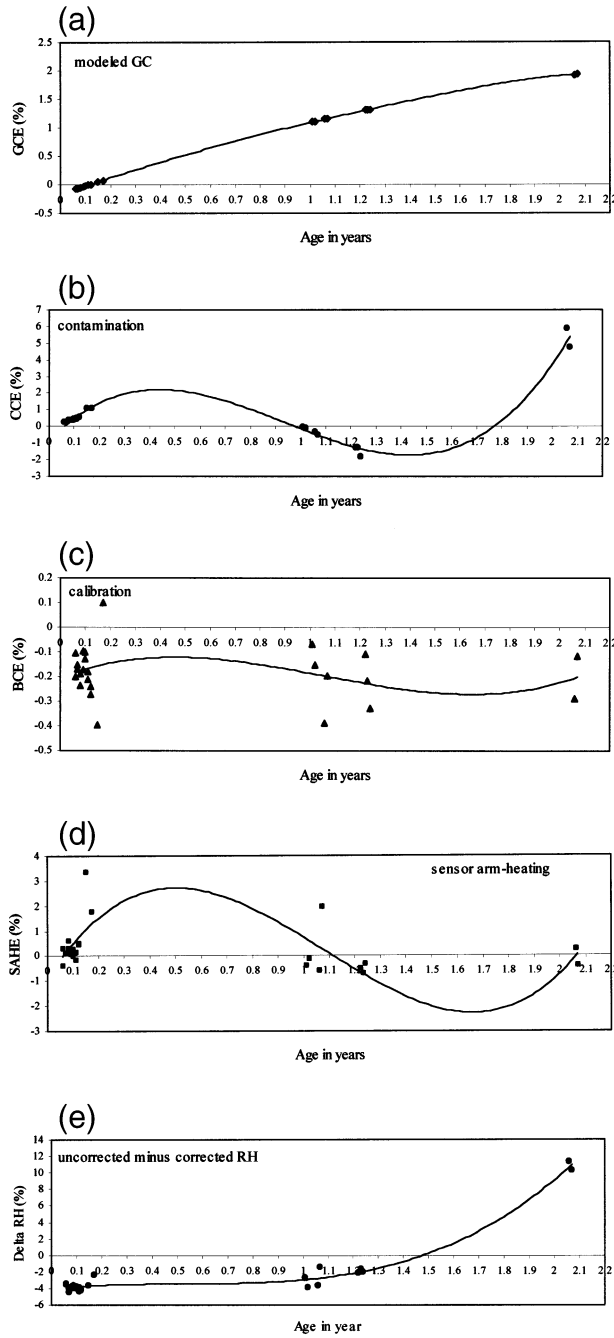


FIG. 7. Variation of model-derived mean correction (%) with sonde age: modeled GCE, modeled CCE, modeled SAE, sensor-arm-heating error (at surface), and the uncorrected minus corrected RH data (delta-RH) with sonde age. The curved line in each plot is the trend line added using a sixth-order polynomial fit to the data.

old. In the plot shown in Fig. 8a each point represents an average of all five DSAH-10s data obtained per sounding. There are outliers in the set, but considering all the points together it is noted that both SAHE and DSAH-10s bear a sinusoidal function of age. The period noted from this plot is close to 2 yr. Even after removing

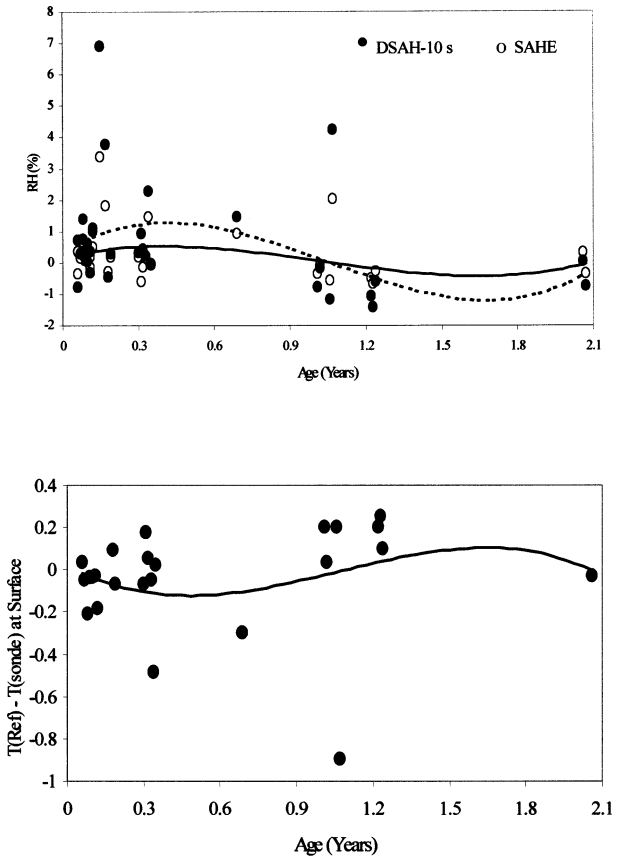


FIG. 8. (top) Variation of mean SAHE (and DSAH10-s) with sonde age. (bottom) Variation of mean of the difference of surface reference temperature and sonde surface temperature with sonde age.

the DSAH-10s outliers the sinusoidal pattern is preserved. A spline fit (Press et al. 1992) of SAHE and DSAH-10s with age could be obtained:

$$SAHE = 2.43d^3 - 7.6d^2 + 5.08d + 0.3 \quad (10)$$

$$DSAH-10s = 0.96d^3 - 2.95d^2 + 1.88d + 0.2. \quad (11)$$

A closer look suggests that the reference temperature obtained at surface and the sonde surface temperature used for calculating the surface saturation vapor pressure in (8a) give rise to such a sinusoidal variation of SAHE with age of sonde. Evaluating the ratio $e_s(T_{sr})/e_s(T_{ss})$ in (8a) by using the Bolton (1980) method and using a common reference surface pressure, the ratio of vapor pressure could be written as

$$\frac{e_{sr}}{e_{ss}} = \frac{\exp[(T_{sr}a)/(T_{sr} + b)]}{\exp[(T_{ss}a)/(T_{ss} + b)]} \quad \text{or} \quad (12)$$

$$\log_e \left[\frac{e_{sr}(T_{sr})}{e_{ss}(T_{ss})} \right] = \frac{a(T_{sr} - T_{ss})}{(T_{sr} + b)(T_{ss} + b)}, \quad (13)$$

where $a = 17.67$ and $b = 243.5$. It is evident from (13) that the ratio of saturation vapor pressure in (8a) depends upon the difference in measured surface temperature.

TABLE 1. The number of radiosonde launches at each site, the number of soundings that exceed the 800 J Kg^{-1} threshold before and after W02 correction, and the site-mean CAPE for each station. The percentage improvement (% increase) in site-mean CAPE and the mean of % RH improved (mean moisture-loading) with respect to the old estimates are also mentioned for each site.

Site	Number of soundings	Number of soundings CAPE > 800 J Kg^{-1}		Site-mean CAPE (J Kg^{-1})		
		Before	After RH correction	Before	After RH correction	Improvement
Rebio-Jaru	217	100	109	790	889	13%
Rolim de Moura	190	82	102	757	933	23%
R/V <i>RHB</i>	281	175	240	824	1728	109%
		Mean daytime RH error correction		Mean nighttime RH error correction		
Rebio-Jaru		2.0%		2.1%		
Rolim de Moura		2.1%		2.8%		
R/V <i>RHB</i>		5.0%		10.7%		

Figure 8b shows variation of the difference between the independently measured surface temperature and the radiosonde surface temperature, with sonde age. The nature of variation between the temperature error and SAHE with age are just opposite (cf. Figs. 8a and 8b). A decrease in temperature error will increase the SAHE error in RH for the first 50 s, and vice versa. If we truly represent the surface reference temperature with frequency ω_1 and phase ϕ_1 , and the surface sonde temperature with frequency ω_2 and phase ϕ_2 , having amplitudes B_1 and B_2 , respectively, then

$$T_{rs} = B_1 \cos(\omega d + \phi_1) \quad (14)$$

$$T_{ss} = B_2 \cos(\omega d + \phi_2). \quad (15)$$

If we now take the difference in temperature with amplitude A as a cosine function of age with the same frequency but with a phase ϕ ,

$$T_{rs} - T_{ss} = A \cos(\omega d + \phi), \quad (16)$$

then from (15) and (16) we get

$$T_{rs} = B_2 \cos(\omega d + \phi_2) + A \cos(\omega d + \phi). \quad (17)$$

Rearranging and using the identity $\cos[2(\omega d + \phi_2)] = [2 \cos^2(\omega d + \phi_2) - 1]$ and simplifying this further for condition $\phi_2 \approx \phi$, we could write the denominator of (11) as

$$(T_{sr} + b)(T_{ss} + b) = P \cos(\omega d + \phi_3). \quad (18)$$

Hence the right-hand side of (13) could be written in terms of the modified amplitude and phase:

$$\begin{aligned} \frac{a(T_{sr} - T_{ss})}{(T_{sr} + b)(T_{ss} - b)} &= \frac{aA \cos(\omega d + \phi)}{D \cos(\omega d + \phi_3) + K} \\ &= P' \cos(\omega d + \phi_4), \end{aligned} \quad (19)$$

where

$$K = b^2 + \frac{B_2 A}{2}.$$

From (19) it is evident that the ratio behaves as a cosine function with sonde age but with a combined phase and

amplitude. The mean surface temperature error could be approximately represented as a function of sonde age while using a spline fit of the data:

$$T_{rs} - T_{ss} = -0.3d^3 + 0.9d^2 - 0.7d + 0.023. \quad (20)$$

d. Improvement in CAPE

CAPE is the measure of maximum work done by buoyancy and is obtained by integrating the differences in the virtual temperature of parcel ($T_{v\text{-parcel}}$) and that of surrounding ($T_{v\text{-surr}}$) overall pressure levels in the region between the level of free convection (LFC; where the parcel become positively buoyant) and the level of neutral buoyancy (LNB; the height at which the parcel regains stability) as mentioned in Bohren and Albrecht (1998):

$$\text{CAPE} = -R_d \int_{\text{LFC}}^{\text{LNB}} (T_{v\text{-parcel}} - T_{v\text{-surr}}) d \ln P. \quad (21)$$

CAPE values were computed once using the uncorrected soundings and again using corrected RH data. The CAPE values for individual soundings show a significant increase after application of the W02 algorithm. This in turn enhanced the LBA and KWAJEX site-mean CAPE. CAPE is very sensitive to temperature and humidity data of the surface parcel. We have seen that application of the W02 algorithm helped modify the boundary layer relative humidity to a great extent, resulting in larger CAPE. Table 1 gives the CAPE increase in percentage of the original values. We also note that the number of soundings that yield CAPE > 800 J kg^{-1} before and after application of the W02 algorithm have increased (see Table 1). We chose 800 J kg^{-1} as a threshold energy level because at this energy convective velocity of the order 40 m s^{-1} could be reached, which is sufficient for convective initiation. This inference is based on a COARE study (LeMone et al. 1998). CAPE was greatly enhanced for the R/V *RHB* soundings. This is justified from Fig. 5, where we have noted that the W02 algorithm improves R/V *RHB* humidity data con-

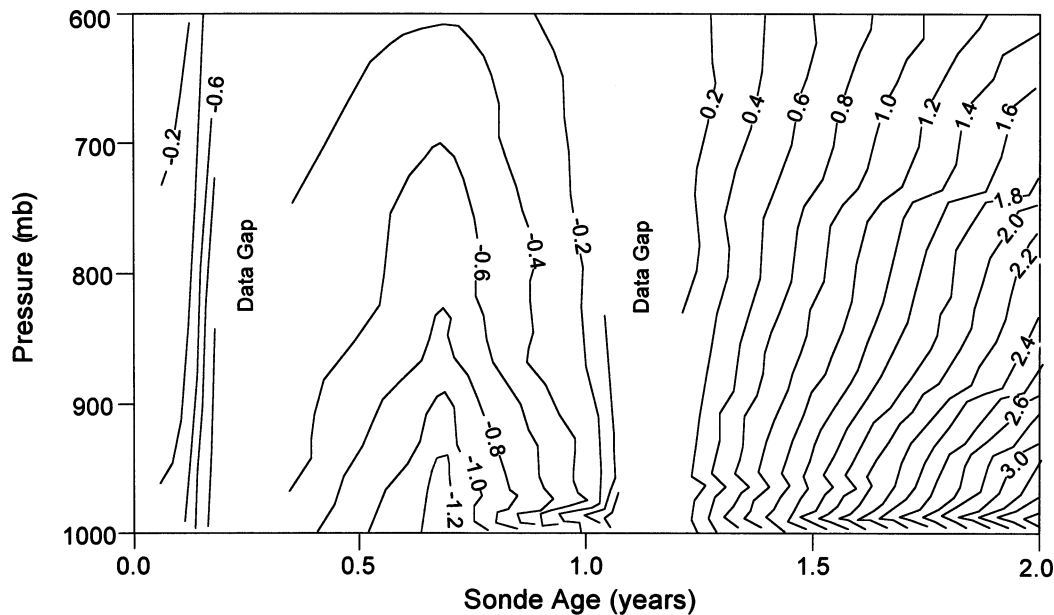


FIG. 9. The age–height plot of specific humidity (g kg^{-1}) difference between uncorrected and W02-corrected RS80-H data. Note that the sign of the contours changes from negative to positive for the sonde age exceeding 1.25 yr.

siderably for the first few hundred meters of the sounding. Obviously, this has resulted in more moistening of the surface parcel and, hence, very large CAPE.

e. Age–height analysis of specific humidity data

Specific humidity was calculated using the Bolton (1988) saturation vapor pressure for the uncorrected and corrected soundings. The differences between uncorrected- and corrected-sounding specific humidity (Δq) for all 709 soundings were plotted in terms of sonde age and levels. The contour plot (Fig. 9) has two distinct data gaps because there were no sondes whose RS80-H sensors were aged to fall in those ranges. It is understood from Fig. 9 that Δq increases with age and also that the specific humidity errors in the original soundings were as high as 3.4 g kg^{-1} when the sondes were about 2 yr old. The contour plot also suggests that the specific humidity errors did not have significant height variation except for the lower regions.

5. Summary

We have successfully corrected all Vaisala soundings taken from various TRMM field campaign sounding sites using the recently published RS80-H system-bias correction algorithm (W02). The sounding environments were essentially of two types: oceanic (R/V *RHB*) and land sites (Rebio-Jaru and Rolim de Moura).

While comparing the mean humidity and temperature profiles obtained using Vaisala soundings at Rebio-Jaru with the VIZ soundings taken at Abracos during the LBA we found a large amount of dry bias in the Vaisala

soundings for the lower levels. Timely publication of the W02 algorithm involving six correction models based on extensive laboratory tests (mentioned in W02) have helped TRMM soundings quality control efforts.

A detailed flowchart showing the W02 algorithm is presented. Use of correction model equations in W02 have been explained in terms of the actual procedure. Most of the W02-model-derived error calculation procedures for GCE, BCE, CCE, and DSAH-10s are similar to those reported in Wang et al. (2002), except in the case of R/V *RHB*, where we have used the IMET-derived 1-min average data for GCE estimation instead of handheld instrument data. CCE was found to be relatively large when compared with all other five errors calculated in the procedure. The uncorrected minus corrected humidity error profile (difference profile) shows negative values, which signifies that more moisture is added to the soundings. We have seen that over the land, as well as over the ocean, W02 adds more moisture to the nighttime soundings than during the daytime soundings. In case of soundings over land (Rebio-Jaru and Rolim de Moura) a large amount of moisture loading occurs above the midlevel after W02 is applied. The shape of the difference profile at the 200–100-mb region shows consistency with the original humidity profile.

Most significant changes are observed in the boundary layer humidity profile. We believe that the positive changes imparted to the humidity data in the boundary layer are justified. The overall humidity corrections resulted in calculation of larger CAPE values and diminished the difference between the mean uncorrected humidity profiles and site-mean humidity profiles (at least we have confirmed this for the R/V *RHB* case). In gen-

eral, we point out that the W02-based corrections are more appropriate for the lower sounding levels.

The difference profile computed for the R/V *RHB* does not show any significant variation with height, unlike those obtained for the land sounding sites. This signifies that the corrections made to the R/V *RHB* site are more consistent. We attribute such a contrast in difference profiles between land and ocean to errors that might be introduced in GCE due to use of handheld instruments for prelaunch surface data acquisition at the land-based (LBA) sites.

Sensor-arm-heating error in the daytime soundings calculated using the method prescribed in the W02 algorithm well suits our corrected products. Further, we have investigated that the actual interpolated SAHE at the successive levels (DSAH-10s) in the first 200–300-m ranges bear a sinusoidal relation with the sonde age. For the purpose of idealization we have shown that the difference between the logarithm of vapor pressure as a function of surface-reference temperature and the logarithm of vapor pressure as a function of sonde-measured temperature bears a cosine function with sonde age and has a combined phase and amplitude. This is being pointed out for the first time. We are suggesting that while using the W02 method for RH correction it might be useful to adjust the difference between surface-reference temperature and sonde-measured temperature in terms of sonde age using a polynomial fit (20).

Site-mean CAPE values have been observed to increase after application of the W02 correction method because the correction is found to adjust the surface-parcel moisture levels in a very appropriate fashion. The specific humidity differences between the uncorrected and W02-corrected soundings show large variation with sonde age (approximately 3.4 g kg^{-1} for 2-yr-old sondes) but no significant variation with height in the upper levels.

These humidity corrections might lead to more efficient mesoscale analysis in line with the large-scale improvements already observed in the TOGA COARE data (Ciesielski et al. 2002, manuscript submitted to *J. Atmos. Sci.*). To check for accuracy of the upper-air data it is advisable that the upper-air corrected RH profiles be compared with some other independent measurements taken during the period of the TRMM field campaigns.

We highly recommend this procedure for RH correction to soundings that were taken using the RS80-H sensor from other sites. In May 2000, Vaisala redesigned and introduced new type of protective shield over the sensor boom for the RS80 sondes, as mentioned in Wang et al. (2002). This prevents outgassing of contaminants to the polymer, hence reducing the chemical contamination level.

The version “e” TRMM Vaisala sounding files have about 367 462 corrected RH observations. These have been posted at the Goddard Distributed Active Archive Center (G-DAAC).

Acknowledgments. The authors wish to acknowledge the support of Dr. Ramesh Kakar (NASA). One of the authors (BR) wishes to thank Dr. George Huffman (SSAI and Laboratory for Atmospheres) and Dr. Dean Duffy (GSFC Laboratory for Atmospheres) for reviewing the manuscript, and Mr. Ken Goss (Vaisala, Inc.) for providing the sonde serial numbers. We also wish to thank TRMM Project Scientist Dr. Robert F. Adler (NASA GSFC) for his continued support in this program.

REFERENCES

- Bohren, C. F., and B. A. Albrecht, 1998: *Atmospheric Thermodynamics*. Oxford University Press, 402 pp.
- Bolton, D., 1980: The computation of equivalent potential temperature. *Mon. Wea. Rev.*, **108**, 1046–1053.
- Cole, H., and E. Miller, 1995: A correction for low-level radiosonde temperature and relative humidity measurements. Preprints, *Ninth Symp. on Meteorological Observations and Instrumentation*, Charlotte, NC, Amer. Meteor. Soc., 32–36.
- Halverson, J. B., T. Rickenbach, B. Roy, H. Pierce, and E. Williams, 2002: Environmental characteristics of convective systems during TRMM-LBA. *Mon. Wea. Rev.*, **130**, 1493–1509.
- Hosom, D. S., R. A. Weller, R. E. Payne, and K. E. Prada, 1995: The IMET (Improved Meteorology) ship and buoy systems. *J. Atmos. Oceanic Technol.*, **12**, 527–540.
- LeMone, M., E. J. Zipser, and S. Trier, 1998: The role of environmental shear and thermodynamic conditions in determining the structure and evolution of mesoscale convective systems. *J. Atmos. Sci.*, **55**, 3493–3518.
- Loehrer, S. M., T. A. Edmunds, and J. A. Moore, 1996: TOGA COARE upper air sounding data archive: Development and quality control procedures. *Bull. Amer. Meteor. Soc.*, **77**, 2651–2671.
- Press, W., S. Teukolsky, W. Vetterling, and B. Flannery, 1992: *Numerical Recipes in the Fortran—The Art of Scientific Computing*. Cambridge University Press, 963 pp.
- Roy, B., and J. B. Halverson, 2002: On quality control procedures being adopted for TRMM LBA and KWAJEX soundings data sets. Preprints, *Symp. on Observations, Data Assimilation, and Probabilistic Prediction*, Orlando, FL, Amer. Meteor. Soc., CD-ROM, P2.6.
- Wallace, J. M., and P. V. Hobbs, 1977: *Atmospheric Science: An Introductory Survey*. Academic Press, 350 pp.
- Wang, J., 2002: Understanding and correcting humidity measurement errors from Vaisala RS80 and VIZ radiosondes. *Proc. Radiosonde Workshop*, Hampton, VA, Center for Atmospheric Sciences, Hampton University, 1–7.
- , H. L. Cole, D. J. Carlson, E. R. Miller, and K. Beierle, 2002: Corrections of humidity measurement errors from the Vaisala RS80 radiosonde-application to TOGA COARE data. *J. Atmos. Oceanic Technol.*, **19**, 981–1002.
- Williams, E., and Coauthors, 2002: Contrasting convective regimes over the Amazon: Implications for cloud electrification. *J. Geophys. Res.*, **107**, 8082, doi:10.1029/2001JD000380.
- Zipser, E. J., and R. H. Johnson, 1998: Systematic errors in radiosonde humidities: A global problem? Preprints, *10th Symp. on Meteorological Observations and Instrumentation*, Phoenix, AZ, Amer. Meteor. Soc., 72–73.